Acta Pharmacol Sin 2008 Apr; 29 (4): 405–412

WILEY-BLACKWELL

Full-length article

Electrophysiological characterization of a novel Kv channel blocker *N*, *N'*-[oxy*bis*(2,1-ethanediyloxy-2,1-ethanediyl)]*bis*(4-methyl)-benzenesulfonamide found in virtual screening[1]

Zhao-bing GAO[2], Xue-qin CHEN[2], Hua-liang JIANG[2,3], Hong LIU[2,3,4], Guo-yuan HU[2,4]

[2]*State Key Laboratory of Drug Research and* [3]*Center for Drug Discovery and Design, Shanghai Institute of Materia Medica, Chinese Academy of Sciences, Shanghai 201203, China*

Key words

blocker; hippocampal neurons; *N*,*N'*-[oxybis (2,1-ethanediyloxy-2,1-ethanediyl)]*bis*(4-methyl)-benzenesulfonamide; patch-clamping recording; virtual screening; voltage-gated K^+ channel

[1]Project supported by research grants from the National Natural Science Foundation of China (No 30472086 and 20472094) and a "863 Hi-Tech Program in China" grant (No 2006AA020602).

[4]Correspondence to Prof Hong LIU and Prof Guo-yuan HU.
Phn 86-21-5080-7042.
E-mail hliu@mail.shcnc.ac.cn (Hong LIU)
Phn 86-21-5080-6778.
E-mail gyhu@mail.shcnc.ac.cn (Guo-yuan HU)

Received 2007-10-30
Accepted 2007-12-23

doi: 10.1111/j.1745-7254.2008.00777.x

Abstract

Aim: *N*,*N'*-[oxybis(2,1-ethanediyloxy-2,1-ethanediyl)]*bis*(4-methyl)-benzenesulfonamide (OMBSA) is a hit compound with potent voltage-gated K^+ (Kv) channel-blocking activities that was found while searching the MDL Available Chemicals Directory with a virtual screening approach. In the present study, the blocking actions of OMBSA on Kv channels and relevant mechanisms were characterized. **Methods:** Whole-cell voltage-clamp recording was made in acutely dissociated hippocampal CA1 pyramidal neurons of newborn rats. **Results:** Superfusion of OMBSA reversibly inhibited both the delayed rectifier (I_K) and fast transient K^+ currents (I_A) with IC_{50} values of 2.1±1.1 μmol/L and 27.8±1.5 μmol/L, respectively. The inhibition was voltage independent. OMBSA markedly accelerated the decay time course of I_K, without a significant effect on that of I_A. OMBSA did not change the activation, steady-state inactivation of I_K, and its recovery from inactivation, but the compound caused a significant hyperpolarizing shift of the voltage dependence of the steady-state inactivation of I_A and slowed down its recovery from inactivation. Intracellular dialysis of OMBSA had no effect on both I_K and I_A. **Conclusion:** The results demonstrate that OMBSA blocks both I_K and I_A through binding to the outer mouth of the channel pore, as predicted by the molecular docking model used in the virtual screening. In addition, the compound differentially moderates the inactivation kinetics of the K^+ channels through allosteric mechanisms.

Introduction

Voltage-gated K^+ (Kv) channels show enormous molecular diversity with approximately 40 pore-forming principal subunits identified that constitute 12 subfamilies (Kv1-Kv12)[1]. The heteromultimeric assembly of different subunits provides a base for further diversity and leads to a huge number of functionally diverse Kvchannels with distinct biophysical, pharmacological, and regulation properties[2]. Increasing evidence shows that the dysfunction of Kv channels is associated with epilepsy, cardiac arrhythmias, skeletal muscle disorders, neurodegenerative diseases, and other diseases[3–5]. Thus, the pharmacological modulation of Kv channels was proposed as a therapeutic strategy in the treatment of disorders[4,6].

High-throughput screening (HTS) technologies have been widely employed to search for drug candidates in pharmaceutical industries. In contrast to those successfully applied in screening enzyme inhibitors or ligands for the G-protein coupled receptor, HTS technologies for ion channel drugs remain a challenge. New methods, such as fluorescence-based assays, radioactive efflux assays, and radiolabeled-ligand binding assays, although representing "industry standards", still rely on conventional patch-clamping recording for assessing the functional interaction of a compound with an ion channel[7,8]. Recently, a variety of prototypes of high-throughput electrophysiology has emerged; however, the throughput is generally low[8,9]. Virtual screening complements bioactivity screening. Nowadays, both ligand- and target-based virtual screening are used as reli-

able methods in the discovery of drug candidates in pharmaceutical industries[10,11]. Based on the crystal structure of the KcsA channel from *Streptomyces lividans*[12], we constructed a 3-D model of a eukaryotic Kv channel and developed a computational virtual screening approach to search large databases for novel Kv channel blockers[13,14]. As a result, we found nearly a dozen hit compounds in both the China Natural Products Database (CNPD) and the MDL Available Chemicals Directory (ACD) that potently inhibited voltage-activated K^+ currents in rat hippocampal neurons.

Several hit compounds have been further characterized with respect to their potency, efficacy and specificity. Among them, OMBSA is the most potent hit compound found in the ACD database[14] (Figure 1). However, it remains unclear whether the hit compound inhibits voltage-activated K^+ currents through the blocking of Kv channels, modification of gating, or shift of voltage dependence[15]. In the present study, the inhibitory effects of OMBSA on voltage-activated K^+ currents in rat hippocampal neurons and the relevant mechanisms were further investigated by using a whole-cell voltage-clamp recording technique.

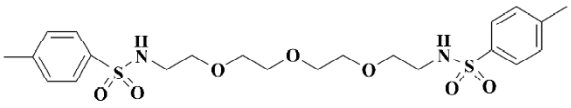

Figure 1. Chemical structure of OMBSA.

Materials and methods

Materials OMBSA (molecular weight 500.1, purity>99.5%) was synthesized in our laboratory. Other chemicals were purchased from Sigma-Aldrich China Inc (China).

Preparation of dissociated hippocampal neurons Sprague-Dawley rats (5–9 d old) were provided by the Shanghai Experimental Animal Center, Chinese Academy of Sciences (Shanghai, China). Dissociated hippocampal neurons were prepared as described previously[16]. Briefly, hippocampal slices (500 μm) were cut in oxygenated ice-cold dissociation solution containing (in mmol/L): 82 Na_2SO_4, 30 K_2SO_4, 5 $MgCl_2$, 10 HEPES, and 10 glucose (pH 7.3 with NaOH). The slices were incubated in dissociation solution containing protease XXIII (3 g/L) at 32 ºC for 8 min, and then placed in dissociation solution containing trypsin inhibitor type II-S (1 g/L) and bovine serum albumin (1 g/L) at 24–25 ºC in an oxygen atmosphere. Before recording, the CA1 regions of several slices were dissected and triturated using a series of fire-polished Pasteur pipettes with decreasing tip diameters. Dissociated neurons were placed in a recording dish and superfused with an external solution containing the following (in mmol/L): 135 NaCl, 5 KCl, 1 $CaCl_2$, 2 $MgCl_2$, 10 HEPES, 10 glucose, and 0.001 tetrodotoxin (pH 7.4 with NaOH).

Whole-cell voltage-clamp recording Voltage-activated K^+ currents were recorded in large, pyramidal-shaped neurons using an Axopatch 200A amplifier (Axon Instruments, CA, USA) at 24–25 ºC. Voltage protocols were controlled by pClamp 9.0 software (Axon Instruments) via a DigiData-1322A interface (Axon Instruments). Recording electrodes (with a tip resistance of 3–5 MΩ) were pulled from borosilicate grass pipettes (Sutter Instruments, USA) and filled with a pipette solution containing the following composition (in mmol/L): 140 KCl, 2 $MgCl_2$, 1 $CaCl_2$, 10 HEPES, and 10 EGTA (pH 7.4 with KOH). Signals were filtered at 2–10 kHz and sampled at frequencies of 10–40 kHz. Series resistance was compensated by 75%–85%. Linear leak and residual capacitance currents were subtracted online using a P/4 protocol.

Drug application OMBSA was dissolved in DMSO to prepare a stock solution of 10 mmol/L and stored at –20°C. The stock solution was diluted to desired concentrations with the external solution before use and applied to the neuron using RSC-100 rapid solution changer with a 9-tube head (BioLogic, France). DMSO (less than 0.1% in the final dilution) had no observed effect on the voltage-activated K^+ currents. For intracellular dialysis, OMBSA in the pipette solution was diffused into the recorded neuron immediately after the patch membrane ruptured[17].

Data analysis The peak amplitude of the fast transient K^+ channel (I_A) was measured, whereas the amplitude of the delayed rectifier channel (I_K) was measured with a 300 ms latency. The decay time constants (τ) of the currents were obtained by fitting the decay time course with a mono-exponential function. The concentrations of OMBSA to yield a 50% block of the K^+ currents (IC_{50}) were obtained by fitting normalized concentration-inhibition relationships to the following equation:

$$I/I_0=1/(1+[\{C\}/IC_{50}]^n),$$

where I_0 and I are current amplitudes measured in the control and in the presence of OMBSA, C is the concentration of OMBSA in the external solution, and n is the Hill coefficient. For analyzing the voltage-dependence of steady-state activation or inactivation of the K^+ currents, normalized conductance or current was plotted against the membrane potential and fitted to the Boltzmann equation:

$$Y=1/(1+\exp[\{V-V_{1/2}\}/k]),$$

where Y is the normalized conductance or current, V is the test potential, $V_{1/2}$ is the voltage at half-maximal activation or inactivation, and k is the slope factor. The time course of recovery of the K^+ currents from inactivation was fitted with a mono-exponential function:

$$I/I_{max}=A*(1-\exp[-\Delta t/\tau]),$$

where I_{max} is the maximal current amplitude, I is the current after a recovery period of Δt, τ is the time constant, and A is the amplitude coefficient. Data are presented as mean±SEM. Statistical significance was assessed using a Student's t-test or one-way ANOVA as appropriate, and $P<0.05$ was considered significant. All analyses were performed using GraphPad Prism 4 (GraphPad Software, Inc, USA) and Excel 2000 software.

Results

Inhibition of voltage-activated K^+ currents by OMBSA in hippocampal neurons As shown in the left panel of Figure 2A, both I_K and I_A were simultaneously recorded from a dissociated pyramidal neuron by using the voltage protocols and a subtraction procedure. Superfusion with OMBSA (30 μmol/L) remarkably reduced the amplitudes of both the voltage-activated K^+ currents elicited by all depolarizing steps (middle panel of Figure 2A). The inhibitory effects had a rapid onset and reached steady-state levels within 10 s. The K^+ currents recovered immediately upon washing out of the compound (Figure 2B, 2C).

In addition to causing a reduction in the amplitude of the I_K, superfusion with OMBSA (30 μmol/L) markedly accelerated the decay of the current (Figure 3A). The τ for I_K was drastically reduced from 271.3±6.2 ms to 23.6±3.9 ms (n=6, $P<0.01$; Figure 3B). In contrast, OMBSA exerted a negligible effect on the decay time course of I_A (Figure 3C). The value of τ for I_A was reduced from 20.9±1.1 ms to 16.5±2.3 ms (n=6), but the change was statistically non-significant ($P>0.05$; Figure 3D). The results suggest that the compound differentially modulated the inactivation of K^+ currents.

Analyses of the concentration-inhibition relationships of OMBSA have revealed that the compound preferentially inhibited I_K to I_A. As shown in Figure 4A, the threshold concentration for the inhibition of I_K was between 0.1 and 1 μmol/L, and I_K was reduced by approximately 90% at 100 μmol/L. In contrast, the threshold concentration for the inhibition of I_A was between 1 and 10 μmol/L, and the amplitude of I_A was reduced by approximately 70% at the maximal concentration tested (300 μmol/L). The IC_{50} value for the inhibition of I_K was 2.1±1.1 μmol/L (Hill coefficient=0.94±0.16, n=6), and that for the inhibition of I_A was 27.8±1.5 μmol/L (Hill coefficient=1.3±0.3, n=6).

Lack of effects of intracellular dialysis of OMBSA on voltage-activated K^+ currents In order to determine the action site of the compound on the Kv channels, the effects of intracellular dialysis of OMBSA on the K^+ currents were investigated. The concentration for intracellular dialysis was 100 μmol/L, which inhibited I_K and I_A by 90% and 65%, respectively, when applied externally (Figure 4A). Throughout the 10 min recording period, the relative amplitudes of I_K and I_A in the neurons dialyzed with OMBSA were almost identical to those in the respective control groups (Figure 4B,4C). At the end of the 10 min recording, the relative amplitude of I_K in the control and in the neurons dialyzed with OMBSA were 89.5%±0.1% and 86.3%±0.1%, respectively (n=6 for each, $P>0.05$); the relative amplitude of I_A in the control and in the neurons dialyzed with OMBSA were 82.7%±0.1% and 92.3%±0.1%, respectively (n=7 for each, $P>0.05$). The results suggest that OMBSA acts at an extracellular site of the Kv channels.

Voltage-independent inhibition of voltage-activated K^+ currents by OMBSA The compound was 13-fold more potent in the inhibition of I_K than of I_A. In order to cause comparable effect on the 2 types of K^+ currents, concentrations of 3 and 30 μmol/L were used for studying I_K and I_A, respectively. The current-voltage (I/V) curves of I_K in the control and in the presence of OMBSA (3 μmol/L) revealed that the compound did not change the threshold for the activation of I_K (Figure 5A). OMBSA apparently caused a linear downward shift of the curve and reduced its amplitude over the entire range of activation.

The relative amplitudes of I_K elicited by depolarizing steps at 0, +20, +40 and +60 mV were 47.7%±8.0%, 49.9%±10.8%, 46.6%±5.1%, and 47.7%±7.6%, respectively (n=7, $P>0.05$, ANOVA; Figure 5B). Similar results were observed for the I/V curve of I_A in the presence of OMBSA (30 μmol/L; Figure 5C). The relative amplitudes of I_A elicited by depolarizing in steps at 0, +20, +40 and +60 mV were 51.4%±5.3%, 52.7%±3.0%, 52.6%±4.0% and 51.5%±4.0%, respectively (n=6, $P>0.05$, ANOVA; Figure 5D). These results demonstrated that the inhibition of I_K and I_A by OMBSA was voltage independent.

Effects of OMBSA on activation and steady-state inactivation of voltage-activated K^+ currents in hippocampal neurons Superfusion of OMBSA (3 μmol/L) had no significant effect on the steady-state activation of I_K, nor did it affect its steady-state inactivation and the time course of recovery from inactivation (Figure 6A,6C,6E). OMBSA (30 μmol/L)

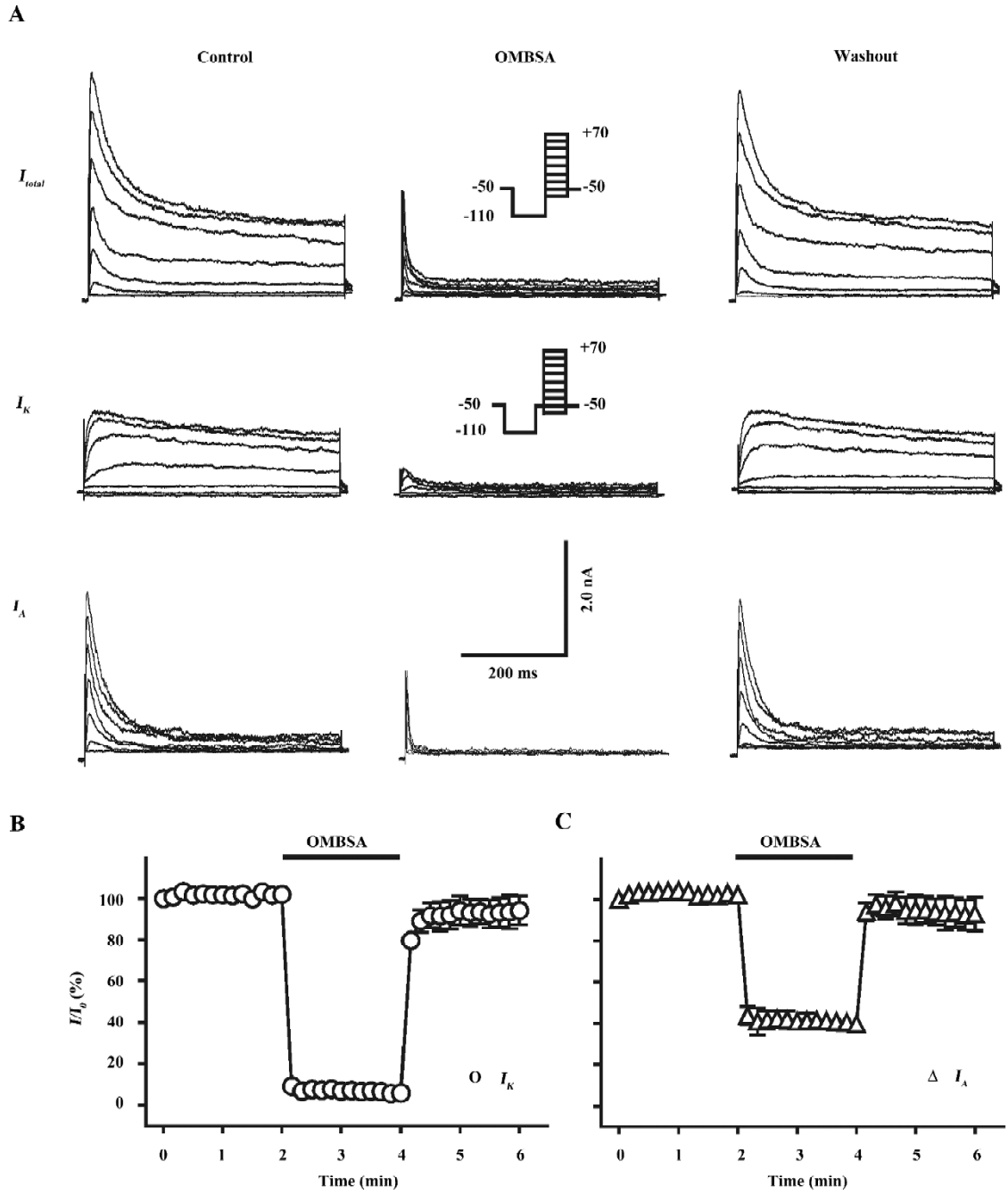

Figure 2. Inhibitory effects of OMBSA on voltage-activated K^+ currents in rat hippocampal neurons. (A) upper, middle, and lower traces are the representative current families of the total K^+ current (I_{total}), I_K and I_A, respectively, before, after 10 s of superfusion with OMBSA (30 μmol/L), and after 10 s of washout. Neuron was held at –50 mV. Upper inset shows the pulse protocol to elicit I_{total}: a 600 ms hyperpolarizing prepulse to –110 mV was followed by a series of 400 ms steps from –70 mV to +70 mV with a 10 mV increment delivered every 10 s. Lower inset shows a similar protocol, but a 50 ms interval at –50 mV was inserted after the prepulse to elicit I_K. I_A is the subtraction of I_K from I_{total}. (B,C) time courses of the inhibition of I_K and I_A by OMBSA (n=3 for each). Bar denotes the superfusion with OMBSA (30 μmol/L). A number of symbols have error bars smaller than their size. Currents were elicited in steps to+40 mV.

had no effect on the voltage dependence of the steady-state activation of I_A, but resulted in a significant hyperpolarizing shift (nearly 8 mV) of its steady-state inactivation curve, and significantly slowed down its recovery from inactivation (Figure 6B,6D,6F). The effects of OMBSA on the kinetic parameters of I_A and I_K are summarized in Table 1.

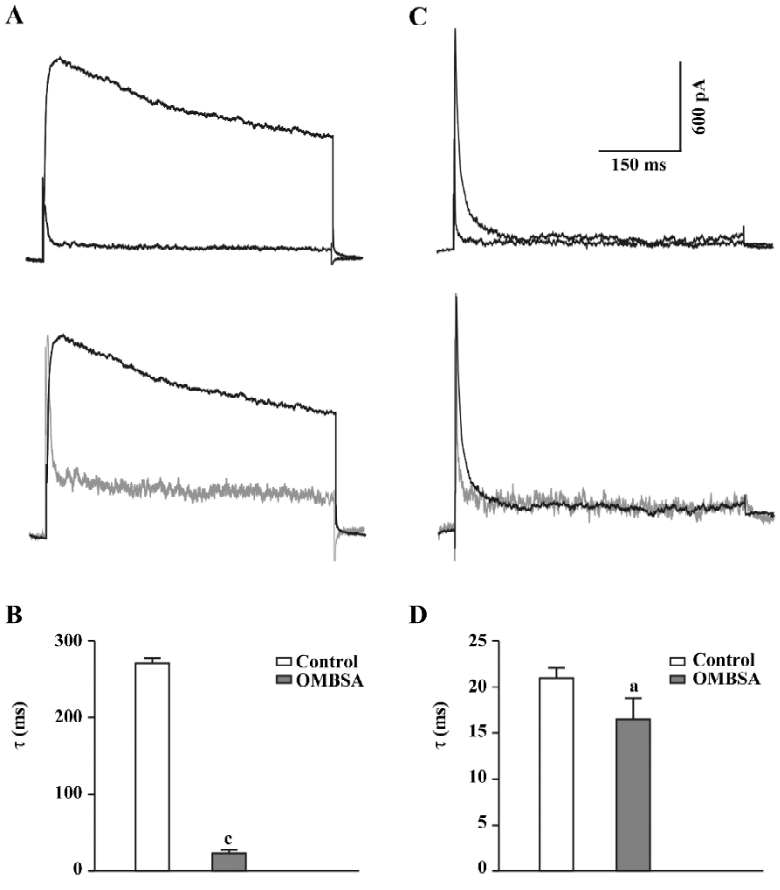

Figure 3. Effects of OMBSA on the decay of I_K and I_A in rat hippocampal neurons. (A) superimposed traces of I_K before and during superfusion with OMBSA (30 μmol/L). At the bottom, the trace with OMBSA is scaled up. (B) decay time constants of I_K before and during superfusion with OMBSA (30 μmol/L). n=6. ^cP<0.01 *vs* the control. (C) I_A before and during superfusion with OMBSA (30 μmol/L) in the same neuron. (D) decay time constants of I_A before and during superfusion with OMBSA (30 μmol/L). n=6. ^aP> 0.05. In the Figure, currents were elicited in steps to +40 mV.

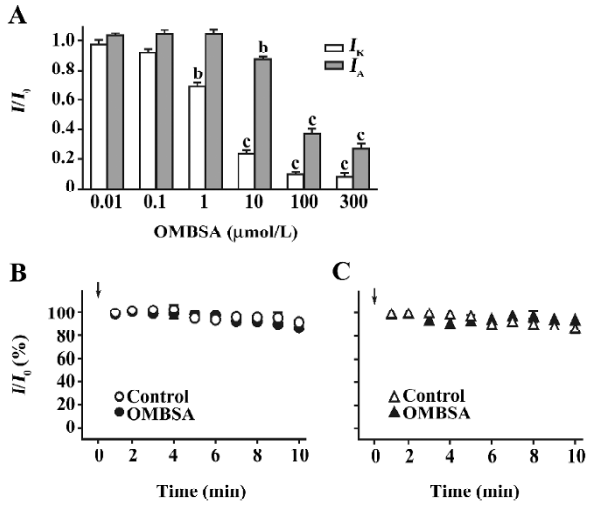

Figure 4. Comparison of the effects of superfusion and intracellular dialysis of OMBSA. (A) concentration-inhibition relationships of OMBSA via superfusion (n=6 for each). ^bP<0.05, ^cP<0.01 *vs* the control. (B,C) lack of effect of intracellular dialysis of OMBSA on the voltage-activated K^+ currents (n=6 for I_K; n=7 for I_A). Recording pipettes were filled with the normal pipette solution and that containing OMBSA (100 μmol/L), respectively. Downward arrows indicate the time when the patch membrane was ruptured. In this Figure, the currents were elicited in steps to +40 mV.

Discussion

Due to the lack of HTS techniques for ion channel drugs[7,9], virtual screening approaches have been developed for discovering new blockers of Kv channels[13,18]. In a virtual screening study[14], a comprehensive assessment of electrostatic and hydrophobic interactions with the Kv channel, and solvation free energy suggests OMBSA to be a hit compound with the most potent Kv channel-blocking activities in the ACD database.

In the present study, we showed that OMBSA potently inhibited both I_K and I_A in rat hippocampal neurons. The compound is 500-fold more potent than tetraethylammonium (TEA) in the inhibition of I_K (the IC_{50} value of TEA was 1.05±0.21 mmol/L[19]), and approximately 180-fold more potent than 4-aminopyridine in the inhibition of I_A (the IC_{50} value of 4-aminopyridine was 4.92±0.65 mmol/L, unpublished data). Furthermore, several interesting clues were found that seemed to be helpful in elucidating the interaction of the compound with Kv channels: (1) the onset of the inhibition and recovery from the inhibition were fast (Figure 2B,2C), suggesting that OMBSA rapidly binds to, and dissociates from the binding site on Kv channels; (2) the inhibition was

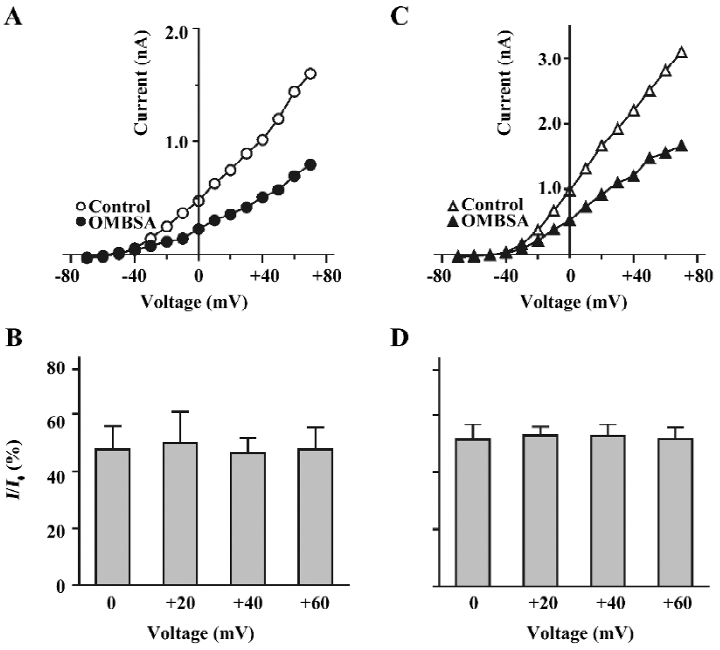

Figure 5. Effects of OMBSA on the *I*/*V* relationships of I_K, and I_A in rat hippocampal neurons. (A) representative *I*/*V* curves of I_K in the control and during superfusion of OMBSA (3 μmol/L). (B) histograms showing the relative amplitude of I_K elicited by different depolarizing steps in the presence of OMBSA (3 μmol/L). Each column is the mean±SEM (n=7). (C) representative *I*/*V* curves of I_A in the control and during superfusion of OMBSA (30 μmol/L). (D) histograms showing the relative amplitude of I_A elicited by different depolarizing steps in the presence of OMBSA (30 μmol/L). Each column is the mean±SEM (n=6).

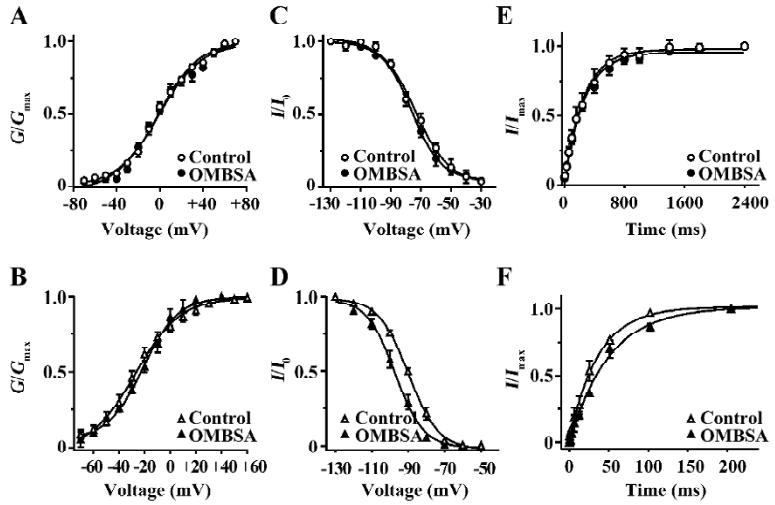

Figure 6. Effects of OMBSA on the activation and steady-state inactivation of voltage-activated K^+ currents in rat hippocampal neurons. (A, C,E) activation curves and steady-state inactivation curves, and the time courses of recovery from the inactivation of I_K, respectively, before and during superfusion with OMBSA (3 μmol/L, n=7 for each). (B,D,F) a set of similar plots for I_A before and during superfusion with OMBSA (30 μmol/L, n=6 for each). Protocols to study the activation are shown in Figure 2A. For studying the steady-state inactivation, neurons were held at 0 mV, and currents were elicited with a series of 600 ms prepulses at different hyperpolarizing potentials followed by a 400 ms step to +40 mV, then back to 0 mV, delivered every 10 s. For studying the time course of recovery from inactivation, the neurons were held at 0 mV, and the currents were elicited on return from hyperpolarizing prepulses of varying durations at –110 mV to +40 mV, delivered every 10 s. In each case, I_K was elicited using a protocol similar to that for I_{total}, but a 50 ms interval at –50 mV was inserted after the prepulse.

voltage independent (Figure 5), which was similar to the blocking of I_K by externally-applied TEA in hippocampal neurons[19]; and (3) intracellular dialysis of OMBSA was ineffective (Figure 4B,4C). The results demonstrate that the compound is most likely to act as a blocker at the outer mouth of the Kv channels, as predicted by the molecular docking model in the virtual screening[13,14]. A similar mechanism has been found for 14-benzoyltalatisamine, a hit compound found in the CNPD database, which selectively blocks I_K through binding to its external pore entry with partial insertion into

Table 1. Effects of OMBSA on kinetic parameters of voltage-gated K^+ channels in rat hippocampal pyramidal neurons. $^bP<0.05$ *vs* respective control.

		Control	OMBSA	*n*
I_K				
Steady-state activation	$V_{1/2}$ (mV)	-0.7±1.3	-1.9±1.9	7
	k (mV^{-1})	18.7±1.4	20.2±2.0	7
Steady-state inactivation	$V_{1/2}$(mV)	-73.7±1.5	-76.2±1.0	7
	k (mV^{-1})	11.3±1.4	9.7±0.9	7
Recovery from inactivation	τ (ms)	235.8±21.7	259.7±12.7	6
I_A				
Steady-state activation	$V_{1/2}$ (mV)	-27.4±2.7	-21.3±1.9	6
	k (mV^{-1})	17.6±2.3	13.7±1.8	6
Steady-state inactivation	$V_{1/2}$ (mV)	-89.8±0.6	-97.2±0.9^b	6
	k (mV^{-1})	-8.3±0.6	-7.8±0.8	6
Recovery from inactivation	τ (ms)	36.4±3.4	49.6±4.1^b	6

Concentrations of OMBSA were 3 and 30 μmol/L, respectively, to study its effects on the kinetic parameters of I_K and I_A. *n*, number of neurons tested.

the selectivity filter[19].

It is also evident that the mode of actions of OMBSA on the 2 types of Kv channels differs: (1) OMBSA is 13-fold more potent in blocking I_K than I_A; (2) OMBSA may bind to I_K with 1:1 stoichiometry (Hill coefficient =0.94±0.16), and to I_A with 2:1 stoichiometry (Hill coefficient =1.3±0.3); and (3) in addition to acting as a channel blocker molecule, OMBSA differentially modulates the kinetics of the Kv channels; it markedly accelerated the inactivation of I_K without significant effect on that of I_A. Moreover, the compound did not change the activation, steady-state inactivation of I_K, and its recovery from inactivation, but caused a significant hyperpolarizing shift of the voltage dependence of the steady-state inactivation of I_A, and slowed down its recovery from inactivation, which led to fewer fast transient K^+ channels available for activation.

In vitro studies have shown that loss of intracellular K^+ ions through enhanced I_K (mainly the Kv2.1 channel) mediates apoptosis of cultured cortical neurons induced by a variety of treatments, and the blocking of the Kv channel reduces neuronal death[20–22]. A number of *in vivo* studies also showed that transient forebrain ischemia resulted in a progressive increase of I_K and a transient upregulation of I_A in hippocampal CA1 pyramidal neurons that led to neuronal injury and programmed cell death[23,24], while blocking I_K by TEA effectively promoted neuronal survival in the CA1 region[25,26]. Recently, the inhibition of an A-type transient K^+ current was found to protect cerebellar granule cells against low K^+/serum deprivation-induced apoptosis[27,28]. Because OMBSA potently blocks both I_K and I_A in hippocampal CA1 pyramidal neurons, it will be interesting to test whether the compound possesses neuroprotective effects.

References

1 Gutman GA, Chandy KG, Adelman JP, Aiyar J, Bayliss DA, Clapham DE, *et al*. International Union of Pharmacology. XLI. Compendium of voltage-gated ion channels: potassium channels. Pharmacol Rev 2003; 55: 583–6.

2 Coetzee WA, Amarillo Y, Chiu J, Chow A, Lau D, McCormack T, *et al*. Molecular diversity of K^+ channels. Ann N Y Acad Sci 1999; 868: 233–85.

3 Curran ME. Potassium ion channels and human disease: phenotypes to drug targets? Curr Opin Biotech 1998; 9: 566–72.

4 Shieh CC, Coghlan M, Sullivan JP, Gopalakrishnan M. Potassium channels: molecular defects, diseases, and therapeutic opportunities. Pharmacol Rev 2000; 52: 557–93.

5 Wickenden AD. K^+ channels as therapeutic drug targets. Pharmacol Therapeut 2002; 94: 157–82.

6 Zaks-Makhina E, Kim Y, Aizenman E, Levitan ES. Novel neuroprotective K^+ channel inhibitor identified by high-throughput screening in yeast. Mol Pharmacol 2004; 65: 214–9.

7 Xu J, Wang X, Ensign B, Li M, Wu L, Guia A, *et al*. Ion-channel assay technologies: *quo vadis*? Drug Discov Today 2001; 6: 1278–87.

8 Worley J III. Guest editor's introduction: an evolution of electrophysiology. Receptor Channel 2003; 9: 1–2.

9 Willumsen NJ, Bech M, Olesen SP, Jensen BS, Korsgaard MPG, Christophersen P. High throughput electrophysiology: new perspectives for ion channel drug discovery. Receptor Channel 2003; 9: 3–12.

10 Lyne PD. Structure-based virtual screening: an overview. Drug Discov Today 2002; 7: 1047–55.

11 Shoichet BK. Virtual screening of chemical libraries. Nature 2004; 432: 862–5.

12 Doyle DA, Cabral JM, Pfuetzner RA, Kuo A, Gulbis JM, Cohen SL, *et al*. The structure of the potassium channel: molecular basis of K^+ conduction and selectivity. Science 1998; 280: 69–77.
13 Liu H, Li Y, Song M, Tan X, Cheng F, Zheng S, *et al*. Structure-based discovery of potassium channel blockers from natural products: virtual screening and electrophysiological assay testing. Chem Biol 2003; 10: 1103–13.
14 Liu H, Gao ZB, Yao Z, Zheng S, Li Y, Zhu W, *et al*. Discovering potassium channel blockers from synthetic compound database by using structure-based virtual screening in conjunction with electrophysiological assay. J Med Chem 2007; 50: 83–93.
15 Hille B. Ionic channels of excitable membranes, 2nd ed. Sunderland Massachusetts: Sinauer Associates Inc; 1992.
16 Yu Y, Chen XQ, Cui YY, Hu GY. Electrophysiological actions of cyclosporin A and tacrolimus on rat hippocampal CA1 pyramidal neurons. Acta Pharmacol Sin 2007; 28: 1891–7.
17 Hu GY, Biro Z, Hill RH, Grillner S. Intracellular QX-314 causes depression of membrane potential oscillations in lamprey spinal neurons during fictive locomotion. J Neurophysiol 2002; 87: 2676–83.
18 Pirard B, Brendel J, Peukert S. The discovery of Kv1.5 blockers as a case study for the application of virtual screening approaches. J Chem Inf Model 2005; 45: 477–85.
19 Song MK, Liu H, Jiang HL, Yue JM, Hu GY. Electrophysiological characterization of 14-benzoyltalatisamine, a selective blocker of the delayed rectifier K^+ channel found in virtual screening. Eur J Pharmacol 2006; 531: 47–53.
20 Yu SP, Yeh CH, Sensi SL, Gwag BJ, Canzoniero LMT, Farhangrazi ZS, *et al*. Mediation of neuronal apoptosis by enhancement of outward potassium current. Science 1997; 278: 114–7.
21 Yu SP, Farhangrazi ZS, Ying HS, Yeh CH, Choi DW. Enhancement of outward potassium current may participate in β-amyloid peptide-induced cortical neuronal death. Neurobiol Dis 1998; 5: 81–8.
22 Pal S, Hartnett KA, Nerbonne JM, Levitan ES, Aizenman E. Modulation of neuronal apoptosis by Kv2.1-encoded potassium channels. J Neurosci 2003; 23: 4798–802.
23 Chi XX, Xu ZC. Differential changes of potassium currents in CA1 pyramidal neurons after transient forebrain ischemia. J Neurophysiol 2000; 84: 2834–43.
24 Zou B, Li Y, Deng P, Xu ZC. Alterations of potassium currents in ischemia-vulnerable and ischemia-resistant neurons in the hippocampus after ischemia. Brain Res 2005; 1033: 78–89.
25 Huang H, Gao TM, Gong LW, Zhuang ZY, Li X. Potassium channel blocker TEA prevents CA1 hippocampal injury following transient forebrain ischemia in adult rats. Neurosci Lett 2001; 305: 83–6.
26 Wei L, Yu SP, Gottron F, Snider BJ, Zipfel GJ, Choi DW. Potassium channel blockers attenuate hypoxia- and ischemia-induced neuronal death *in vitro* and *in vivo*. Stroke 2003; 34: 1281–6.
27 Hu CL, Liu Z, Gao ZY, Zhang ZH, Mei YA. 2-Iodomelatonin prevents apoptosis of cerebellar granule cells via inhibition of A-type transient outward K^+ currents. J Pineal Res 2005; 38: 53–61.
28 Hu CL, Liu Z, Zheng XM, Liu ZQ, Chen XH, Zhang ZH, *et al*. 4-Aminopyridine, a Kv channel antagonist, prevents apoptosis of rat cerebellar granule neurons. Neuropharmacology 2006; 51: 737–46.